

The controlled growth and field emission of Sn-doped and undoped AlN nanorods prepared by halide vapor phase epitaxy

Sang-wook Ui, Young-jong Park, Jae-seok Choi and Sung-churl Choi*

Division of Materials Science & Engineering, College of Engineering, Hanyang University, 17 Haengdang-dong, Seongdong-ku, Seoul 133-791, Korea

We report vapor-solid growth of Sn-doped and undoped AlNnanorods on n-type Si(100) wafers by halide vapor phase epitaxy via a non-catalytic vapor-solid (VS) growth mechanism. Pure Al and Sn metal powders were used as starting materials, and the reaction temperature was 700 °C. By controlling the HCl flow rate, we confirmed that the morphology of Sn-doped and undopedAlN changed into thin flims, nanorods and nanoneedles. The Sn-doped and undopedAlNnanorodswere 500 nm in length, and diameters were in the range of 15-100 nm. The Sn-doped and undopedAlNnanorods grew along the c-axis. The turn-on field and threshold electric field were decreased from 4.2 to 3.87 V/μm and 6.4 to 5.73 V/μm by Sn-doping, while the estimated field enhancement factorswere increased from 523 to 917.

Key words: Halide Vapor Phase Epitaxy, Vapor-solid mechanism, Sn-doped AlNnanorods, Field emission.

Introduction

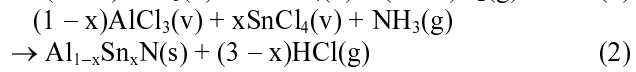
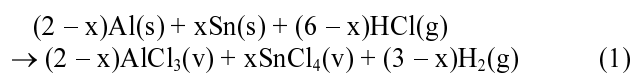
1-dimensional structures of nano-size, such as nanotubes [1], nanobelts [2], nanowires [3, 4] and nanorods [5, 6], have recently attracted much attention for promising applications in optoelectric, biological, and electronic areas. 1-dimensional structures have been prepared based on a catalytic reaction through a vapor-liquid-solid (VLS) growth mechanism [7-9] or a non-catalytic reaction, which is a vapor-solid (VS) growth mechanism [10, 11]. To fabricate 1-dimensional structures, methods such as molecular beam epitaxy [12, 13], chemical vapor deposition [15, 16], metal-organic chemical vapor deposition [17-19] and pulsed laser deposition have been used [20]. Semiconductors of group-III nitrides, for instance, InN, GaN and AlN, have attracted interest because of their unique optical, electrochemical, and thermal properties. In particular, AlN has the largest band gap energy (6.2 eV), the highest thermal conductivity, and the lowest electron affinity (~0.6 eV). Therefore, it has been applied to piezoelectricity [21, 22], UV-LED, LD [23, 24], spintronics [25], sensors [26, 27] and field emission devices [28, 29]. In addition, the AlN nanostructures' tip-size particularly affects the field emission property. The field emission of a separate electron from the tip can influence the local electric field due to the small number of electrons in the tip volume. Furthermore, the field emission property can be enhanced through some dopants, so that the other groups develop enhanced field emission properties by Si doping [30, 31].

In this study, we report the growth of Sn-doped and undopedAlNnanorods by halide vapor phase epitaxy via a non-catalytic vapor solid (VS) growth mechanism. Moreover, the field emission properties of Sn-doped AlN nanostructures are expected to be better than the properties of undopedAlN nanostructures.

Experimental

Growth and V-S mechanism

Sn-doped and undopedAlNnanorods were grown on n-type Si (100) wafers without a catalyst. Pure Al (1.0 g, 200 mesh, 99.0%) and Sn (1.0 g, 100 mesh, 99.5%) metal powders were used as the starting materials. Moreover, N₂ gas served as the carrier gas, and HCl and NH₃ gases were used as the reaction gases. We used two quartz tubes as the reaction tubes, and each tube consisted of an inner and an outer tube. The metal powders were put into the small inner quartz tube. Then, the metal powders were put into the hot zone in the furnace. The substrate was placed in the quartz tube 3.5 cm away from the source materials. To remove remaining air and oxygen, N₂ at 410 sccm was introduced into the quartz tube. The temperature of the furnace was increased 40 K·minute⁻¹ up to 700 °C. The reaction lasted for 15 minute and the temperature was kept at 700 °C. In the end, the temperature of the furnace cooled naturally to 25 °C. Finally, the overall reactions for the formation of AlN :Sn species can be expressed as :



*Corresponding author:
Tel : +82-2-2220-0505
Fax: +82-2-2291-6767
E-mail: choi0505@hanyang.ac.kr

The V-S mechanism has not been investigated until now, but some researchers have suggested theories about the V-S mechanism. According to Kwon [12], the V-S mechanism consists of 6 steps.

The precursor is deposited on the substrate and nucleation occurs. After nucleation on the substrate, small nuclei move to big nuclei and nuclei grow by Ostwald ripening. Once the growing nuclei approach the thermodynamic size limit, a relatively slow reactant supply leads to 1-dimensional structural growth. On the other hand, the formation of AlNnanorods can be roughly divided into 2 steps in our case. First, a large number of AlN move to the surface of the substrate when a high flow rate of carrier gas is applied. The AlN buffer layer is formed by gathering clusters on the surface area at the given process temperature. Second, the transportation rate of AlN clusters slows down in the neck roughly between clusters. In this case, the clusters deposit on nucleation sites and tend to grow into 1-dimensional nano structures through atomic diffusion [32, 33]. Finally, the simultaneous 1-dimensional growth of high-density nuclei forms the array of nanorods. A similar process comprised of the initial growth of a buffer layer and the subsequent growth of nanorods has been observed in our research [33, 34].

Characterization with XRD, FESEM, EDS, HRTEM, and FE

The samples were characterized by diverse methods including x-ray diffraction(XRD; Rigaku, Cu-K α), field emission scanning electron microscopy(FE-SEM; JEOL-7200)equipped with an energy-dispersive X-ray spectrometer(EDS) detector, and high resolution transmission electron microscopy(HRTEM; Tecnai G2 F30). The field emission measurements were carried out using two parallel ITO glassplates in a vacuum system at 5×10^{-6} Torr (6.66612×10^{-11} MPa).

Results and Discussion

Fig. 1 shows a typical XRD pattern for the AlNnanorods with different Sn concentrations. All the diffraction peaks can be indexed to hexagonal wurtzite structured AlN with lattice constants of $a = 3.111 \text{ \AA}$ and $c = 4.979 \text{ \AA}$ (JCPDS No. 25-1133). The strong intensity of the (002) peak indicates that AlN grew along the c-axis. The peak position shifted to higher angles as the Sn content increased (see the inset of Fig. 1). The incorporation of 0.39 at% Sn led to a decrease of the c-plane lattice constant from 4.98 \AA in the undopedAlN to 4.945 \AA . This suggests that the incorporation of Sn ions into the AlNmatrix, as reported in Cr-, Cu-, and V-doped AlN [35-37].

As shown in Fig. 2(A)-(C), when the flow rate of hydrogen chloride was changed significantly different diameters of AlNnanorods were observed .When the flow rate of hydrogen chloride was increased, the diameter of AlNnanorodswas decreased 100 nm, 25 nm and 15 nm. The above results indicate that the diameters of the AlNnanorods

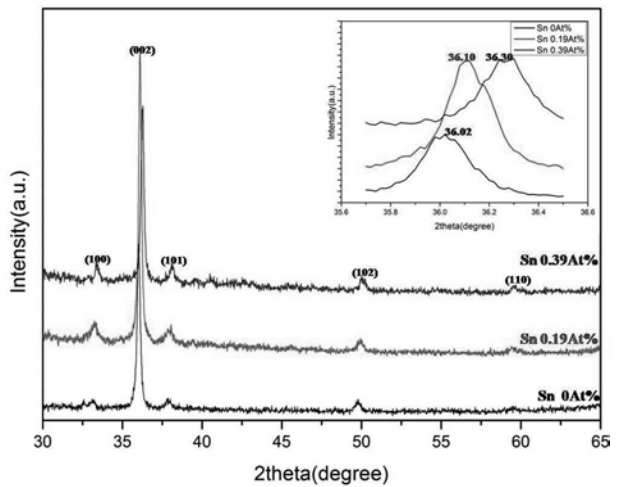


Fig. 1. X-ray diffraction patterns of $\text{Sn}_x\text{Al}_{1-x}\text{N}(x = 0, 0.19, 0.39 \text{ at}\%)$ nanorods grown on Si(100) substrates. The inset figure shows the variation of (002) AlN peak position as the Sn content increases.

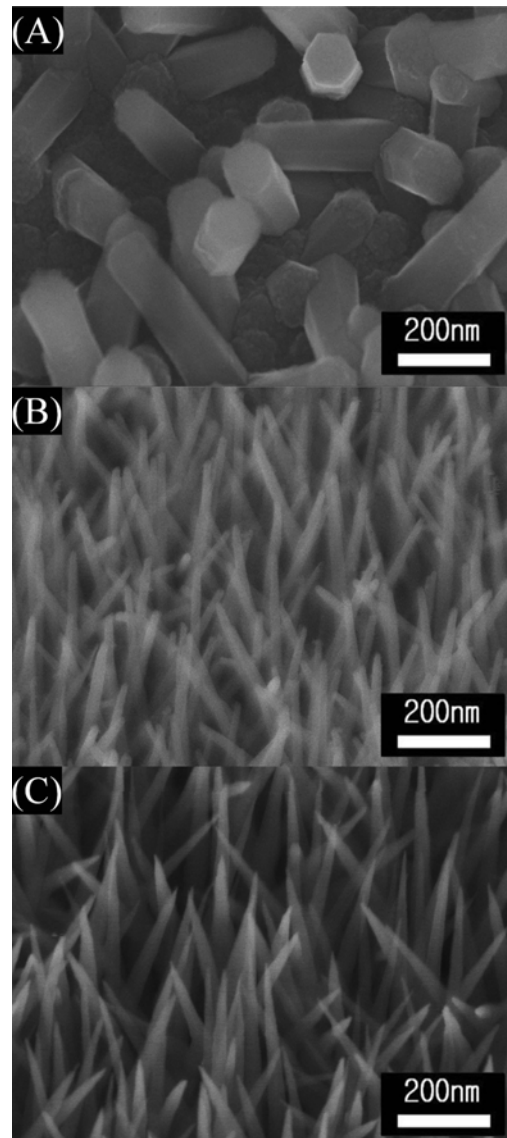


Fig. 2. FESEM images of the products obtained at different HCl flow rates : (A) 15 sccm, (B) 25 sccm, (C) 40 sccm.

can be controlled by tuning the HCl flow rate. The amount of HCl gas has a decisive effect on the nucleation rate. As stated earlier, AlCl₃ reacted between Al precursors and HCl. The AlCl₃ vapor increases with an increase in the HCl flow rate in the HVPE system. When the AlCl₃ vapor is increased more and more, the nucleation rate will be high. The results not only confirm our speculation but also provide us with an effective tool to control the morphology of the AlNnanorods on the substrates.

Fig. 3(A)-(C) show FESEM images, with different amounts of Sn in the AlNnanorods, and other factors (temperature, time, gas flow rate) were fixed. As a result, the morphology was not changed through doping. The samples were Sn-doped and undoped AlNnanorods with a diameter and length of around 25 nm and ~500 nm. Fig. 3(D)-(F) shows that the concentration of the Sn was estimated to be 0-0.39% by the energy dispersive X-ray spectrometer attached to the FESEM.

The structural characterization of Sn-doped and undoped AlNnanorods was carried out by HRTEM, as shown in Fig. 4. The inset of Fig. 4(A) shows the corresponding selected-area electron diffraction (SAED) pattern. This shows that the AlNnanorod is indeed a single crystal. Fig. 4(B) shows a high-resolution TEM(HRTEM) image of a AlNnanorod, showing clear and perfect lattice fringes. The HRTEM image of the lower part of the nanorod (Fig. 4(B)) indicates that the nanorod is a single crystall with an interplanar spacing of 0.498 nm, which is in agreement with the characteristics of the (001) planes of hexagonal AlN. Fig. 4(C)-(D) show HRTEM images of the Sn-doped AlNnanorod. The lattice spacing of 0.245nm is in the growth direction corresponding to the (002) plane of hexagonal AlN. Lattice distortions and nanoclusters can be identified in Fig. 4(C) and (D). The lattice defects suggest the incorporation of Sn ions in the lattice.

The field emission measurements for the Sn-doped and

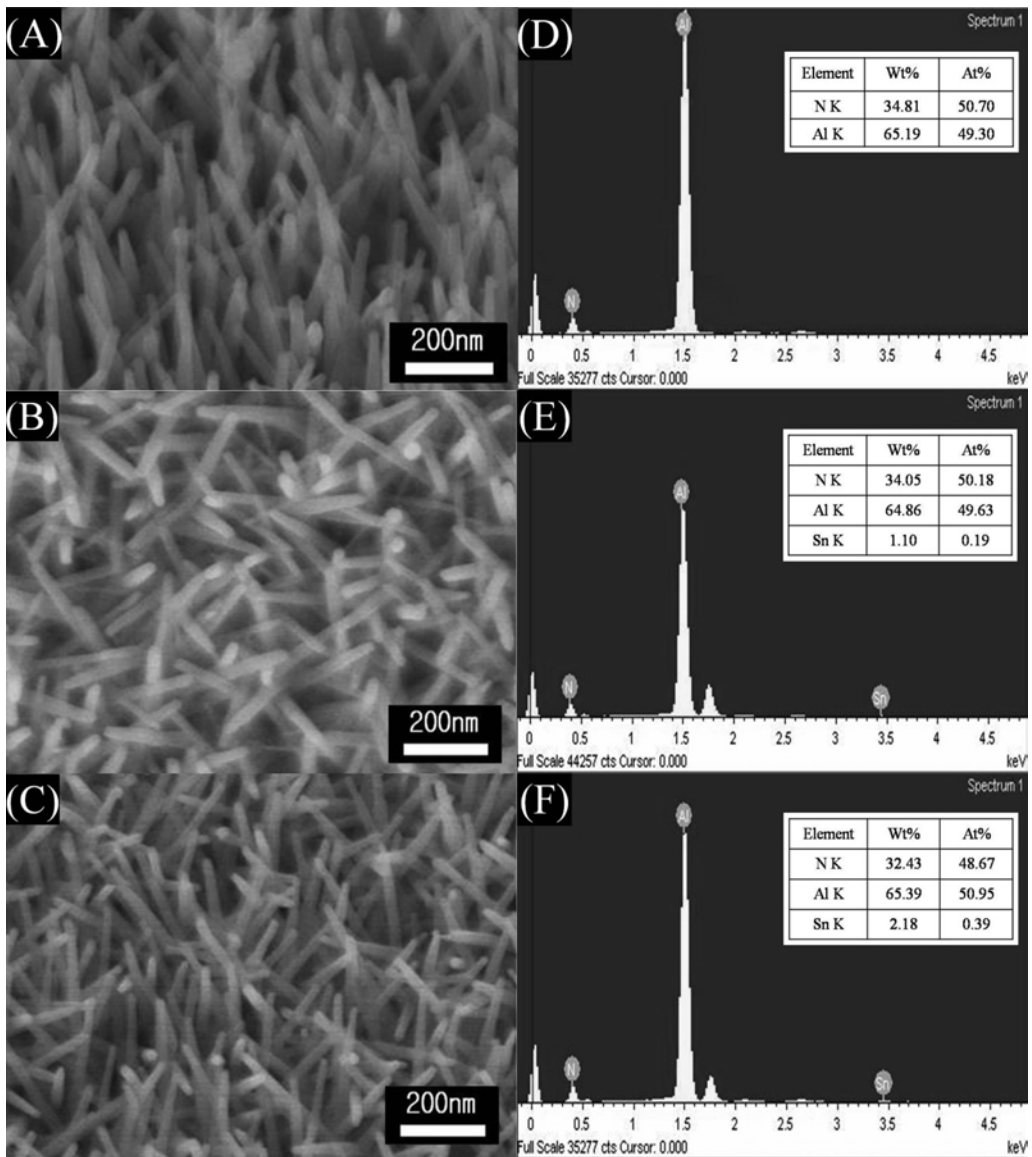


Fig. 3. FESEM image and EDS analysis of the products obtained with different amounts of Sn : (A) and (E) 0 g, (B) and (D) 0.5 g, (C) and (F) 1.0 g.

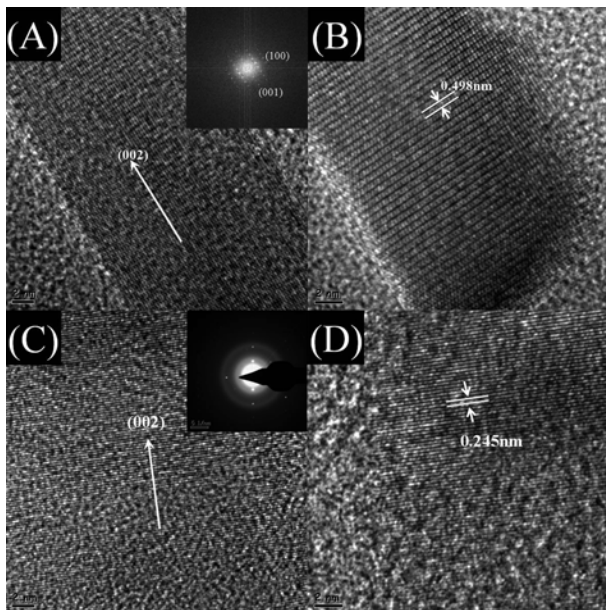


Fig. 4. HRTEM images of Sn-doped and undoped AlN nanorods : (A) and (B) undoped AlN nanorods, (C) and (D) Sn-doped AlN nanorods.

undoped AlN nanorods on Si substrates were performed using two parallel ITO coated glass plates configured in a vacuum chamber. The Sn-doped and undoped AlN nanorods on Si substrates work as the cathode, and the other parallel ITO coated glass operates as the anode. The sample-anode distance was 100 μm . Fig. 5 shows the FE current density as a function of the applied field as a current density versus electric field ($J-E$) plot, and the inset shows a $\ln(J/E^2)$ of the Sn-doped and undoped AlN nanorods. The well-aligned Sn-doped and undoped AlN nanorods have excellent turn-on field values. The turn-on field (defined as the electric field required to operate a current density of 0.01 mA/cm^2) of Sn-doped AlN nanorods was found to be about $3.87 \text{ V}/\mu\text{m}$,

while the value for undoped AlN nanorods was $4.2 \text{ V}/\mu\text{m}$. The threshold fields (defined to be the electric field required to operate a current density of 1 mA/cm^2) of Sn-doped and undoped AlN nanorods were around $5.73 \text{ V}/\mu\text{m}$ and $6.4 \text{ V}/\mu\text{m}$, respectively. It is concluded that Sn-doped AlN nanorods have smaller turn-on field and threshold field. The inset of Fig. 5 shows the corresponding Fowler-Nordheim (F-N) plots of the field emission of the Sn-doped and undoped AlN nanorods. Each F-N plot shows a linear dependence, which reveals that the emission current is obviously caused by the quantum tunneling effect. Based on the Fowler-Nordheim theory, the relationship between current density J and applied electric field E can be described as follows[38]:

$$J = (A\beta^2 E^2/\phi) \exp\left[-\frac{B\phi^{3/2}}{(\beta E)}\right] \quad (3)$$

where $A = 1.54 \times 10^{-10} (\text{AV}^{-2}\text{eV})$, $B = 6.83 \times 10^9 (\text{Vm}^{-1}\text{eV}^{-3/2})$, and ϕ is the work function, which is estimated to be 3.7 eV for AlN [36]. In the equation, β is the field enhancement factor, which can be determined through the F-N plots. The β value of Sn-doped and undoped AlN nanorods were calculated to be around 917 and 523, respectively. It can be suggested that the β value is dependent on the dopant. AlN can be n-type through Si or Sn doping. The dopant will form an impurity level below the conduction band of AlN. Therefore, the electrons for FE can easily tunnel through this shallow donor level to the vacuum under an electric field [39]. The results indicate that the Sn-doped AlN nanorods obtained are indeed a good candidate as field emitters in field-emission devices.

Conclusions

In conclusion, Sn-doped and undoped AlN nanorods were synthesized by halide vapor phase epitaxy with a vapor-solid mechanism. The Sn-doped and undoped AlN nanorods grew along the c-axis. A vapor-solid growth mechanism was proposed to explain the possible formation. The diameter and morphology of undoped and Sn-doped AlN nanorods were controlled through changing the HCl flow rate. These nanorods have lengths up to 500 nm and diameters in the range of $15\text{-}100 \text{ nm}$. A difference in field emission characteristics between Sn-doped and undoped AlN nanorods was observed. Sn-doped AlN nanorods have a lower turn-on field ($3.87 \text{ V}/\mu\text{m}$) and higher β (917) than the value for undoped AlN nanorods. Therefore, the field emission properties of Sn-doped AlN nanorods have potential applications as electron emitter materials in field emission devices.

Acknowledgement

This work was supported by the research fund of Hanyang University (HY-2007-I).

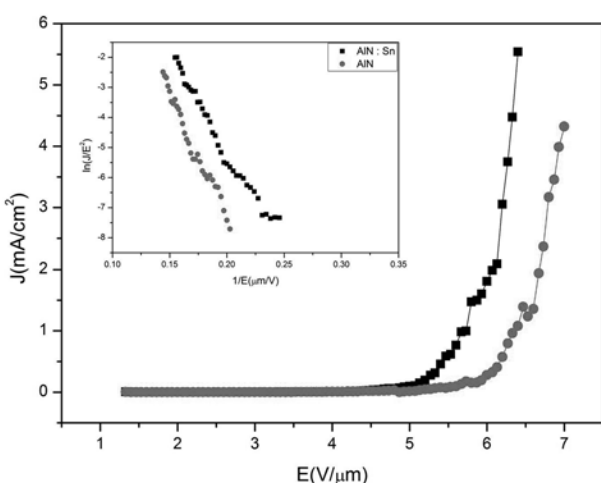


Fig. 5. Field emission current density versus electric field ($J-E$) for Sn-doped and undoped AlN nanorods. The inset shows the corresponding Fowler-Nordheim relationship ($\ln(J/E^2)-1/E$ plot).

References

1. Q. Wu, Z. Hu, X. Wang, Y. Lu, X. Chen, H. Xu and Y. Chen, *J. Am. Chem. Soc.* 125 (2003) 10176.
2. Q. Wu, Z. Hu, X. Wang and Y. Chen, *J. Phys. Chem. B.* 107 (2003) 9726.
3. M. Lei, B. Song, X. Guo, Y.F. Guo, P.G Li and W.H. Tang, *J. Eur. Ceram. Soc.* 29 (2009) 195.
4. Q. Zhao, H.Z. Zhang, X.Y. Xu, Z. Wang, J. Xu and D.P. Yu, *Appl. Phys. Lett.* 86 (2005) 193101.
5. J.H. He, R.S. Yang, Y.L. Chueh, L.J. Chou, L.J. Chen and Z.L. Wang, *Adv. Mater.* 18 (2006) 650.
6. X.H. Ji, Q.Y. Zhang, Z.Y. Ling and S.P. Lau, *Appl. Phys. Lett.* 95 (2009) 233105.
7. Q. Wu, Z. Hu, X. Wang, Y. Lu, K. Huo, S. Deng, N. Xu, B. Shen, R. Zhang and Y. Chen, *J. Mater. Chem.* 13 (2003) 2024.
8. J.H. Duan, S.G. Yang, H.W. Liu, J.F. Gong, H.B. Huang, X.N. Zhao, R. Zhang and Y.W. Du, *J. Phys. Chem. B.* 109 (2005) 3701.
9. Y. Wu and P. Yang, *J. Am. Chem. Soc.* 123 (2001) 3165.
10. P. Yang and C.M. Lieber, *Science*. 273 (1996) 1836.
11. S.J. Kwon, *J. Phys. Chem. B.* 110 (2006) 3876.
12. R. Calarco, R.J. Meijers, R.K. Debnath, T. Stoica, E. Sutter and H. Luth, *Nano lett.* 7 (2007) 2248.
13. L.W. Tu, C.L. Hsiao, T.W. Chi and K.Y. Hsieh, *Appl. Phys. Lett.* 82 (2003) 1601.
14. J. Yang, T.W. Liu, C.W. Hsu, L.C. Chen, K.H. Chen and C.C. Chen, *Nanotechnol.* 17 (2006) S321.
15. X. Song, Z. Guo, J. Zheng, X. Li and Y. Pu, *Nanotechnol* 19 (2008) 115609.
16. V. Cimalla, C. Foerster, D. Cengher, K. Tonisch and O. Ambacher, *Phys. Stat. sol. (b)* 243 (2006) 1476.
17. M. Tchernycheva, C. Sartel, G. Cirlin, L. Travers, G. Patriarche, L. Largeau, O. Mauguin, J.C. Harmand, L.S. Dang, J. Renard, B. Gayral, L. Nevou and F. Julien, *Phys. stat. sol. (c)* 5 (2008) 1556.
18. T. Okada, B.H. Agung and Y. Nakata, *Appl. Phys. A* 79 (2004) 1417.
19. Y. Sun, G.M. Fuge and M.N.R. Ashfold, *Chem. Phys. Lett.* 396 (2004) 21.
20. M. Dubois and P. Muralt, *Appl. Phys. Lett.* 74 (1999) 3032.
21. H.P. Loebi, M. Klee, C. Metzmacher, W. Brand, R. Milsom and P. Lok, *Mater. Chem. Phys.* 79 (2003) 143.
22. Y. Taniyasu, M. Kasu and T. Makimoto, *Nature* 325 (2006) 325.
23. K.B. Nam, J. Li, M.L. Nakarmi, J.Y. Lin and H.X. Jiang, *Appl. Phys. Lett.* 84 (2004) 5264.
24. M. Simeoni, S. Santucci, S. Picozzi and B. Delley, *Nanotechnol.* 17 (2006) 3166.
25. K. Ou, C. Chen, C. Lin, C. Chen, C. Lin and S. Lee, *J. Electrochem. Soc.* 154 (2007) P11.
26. Z. Zhou, J. Zhao, Y. Chen, P.R. Schleyer and Z. Chen, *Nanotechnol.* 18 (2007) 424023.
27. V.N. Tondare, C. Balasubramanian, S.V. Shende, D.S. Joan, V.P. Godbole and S.V. Bhoraskar, *Appl. Phys. Lett.* 80 (2002) 4813.
28. J.H. He, R. Yang, Y.L. Chueh, L.J. Chou, L.J. Chen and Z.L. Wang, *Adv. Mater.* 18 (2006) 650.
29. M. Kasu and N. Kobayashi, *J. Crystal Growth*. 221 (2000) 739.
30. Y.B. Tang, H.T. Cong, Z.M. Wang and H.M. Cheng, *Appl. Phys. Lett.* 89 (2006) 253112.
31. J.A. Haber, P.C. Gibbons and W.E. Buhro, *J. Am. Chem. Soc.* 119 (1997) 5455.
32. F.G. Tarntair et al, *Appl. Phys. Lett.* 76 (2000) 2630.
33. L.C. Chen, S.W. Chang, C.S. Chang, C.Y. Wen, J.J. Wu, Y.F. Chen, Y.S. Huang and K.H. Chen, *J. Phys. Chem. Solid* 62(2001) 1567.
34. A.Y. Polyakov, N.B. Smirnov, A.V. Govorkov, R.M. Frazier, J.Y. Liefer, G.T. Thaler, C.R. Abernathy, S. Pearton and J.M. Zavada, *Appl. Phys. Lett.* 85 (2004) 4067.
35. X.H. Ji, S.P. Lau, S.F. Yu, H.Y. Tang, T.S. Herring and J.S. Chen, *Nanotechnol.* 18 (2007) 105601.
36. K.Y. Ko, Z.H. Barber and M.G. Blamire, *Appl. Phys. Lett.* 100 (2006) 083905.
37. R.H. Fowler and G.S. Rushbrooke, *Trans. Faraday Soc.* 33 (1937) 1272.
38. Y. Taniyasu, M. Kasu and T. Makimoto, *Appl. Phys. Lett.* 84 (2004) 2115.